The Astrophysical Journal, 652:1090–1096, 2006 December 1

PROBING THE LOW-LUMINOSITY X-RAY LUMINOSITY FUNCTION IN NORMAL ELLIPTICAL GALAXIES

D.-W. Kim,[1] G. Fabbiano,[1] V. Kalogera,[2] A. R. King,[3] S. Pellegrini,[4] G. Trinchieri,[5] S. E. Zepf,[6] A. Zezas,[1] L. Angelini,[7] R. L. Davies,[8] and J. S. Gallagher[9]

Received 2006 May 30; accepted 2006 August 8

ABSTRACT

We present the first low-luminosity [$L_X > (5-10) \times 10^{36}$ ergs s^{-1}] X-ray luminosity functions (XLFs) of low-mass X-ray binaries (LMXBs) determined for two typical old elliptical galaxies, NGC 3379 and NGC 4278. Because both galaxies contain little diffuse emission from hot ISM and no recent significant star formation (hence no high-mass X-ray binary contamination), they provide two of the best homogeneous sample of LMXBs. With 110 and 140 ks *Chandra* ACIS S3 exposures, we detect 59 and 112 LMXBs within the D_{25} ellipses of NGC 3379 and NGC 4278, respectively. The resulting XLFs are well represented by a single power law with a slope (in a differential form) of 1.9 ± 0.1. In NGC 4278, we can exclude the break at $L_X \sim 5 \times 10^{37}$ ergs s^{-1} that was recently suggested as being a general feature of LMXB XLFs. In NGC 3379, on the other hand, we find a localized excess over the power-law XLF at $\sim 4 \times 10^{37}$ ergs s^{-1}, but with a marginal significance of $\sim 1.6\,\sigma$. Because of the small number of luminous sources, we cannot constrain the high-luminosity break (at 5×10^{38} ergs s^{-1}) found in a large sample of early-type galaxies. For our two galaxies, the ratios of the integrated LMXB X-ray luminosities to the optical luminosities differ by a factor of 4, but are consistent with the general trend of a positive correlation between the X-ray–to–optical luminosity ratio and the globular cluster specific frequency.

Subject headings: galaxies: elliptical and lenticular, cD — X-rays: binaries — X-rays: galaxies

1. INTRODUCTION

Low-mass X-ray binaries (LMXBs) are luminous X-ray sources associated with old stellar populations, powered by the accretion of the atmosphere of a low-mass late-type star onto a compact stellar remnant, either a neutron star or black hole. The formation and evolution of LMXBs has been debated since their discovery in the Galaxy. Proposed evolutionary paths include both native field binary systems and binary formation by dynamical interactions in either the inner bulge or globular clusters (e.g., Grindlay 1984; see reviews in Bildsten & Deloye 2004; Verbunt & Lewin 2006). This debate has been rekindled by the detection of populations of these sources in early-type galaxies with *Chandra*. In these galaxies, a significant fraction of the LMXBs have been found in globular clusters, but there is also some evidence pointing to native field binaries (e.g., Maccarone et al. 2003; Irwin 2005; Kim et al. 2006a and references to earlier work therein; see review by Fabbiano 2006).

The X-ray luminosity function (XLF) of LMXB populations has emerged as a tool with great potential for constraining the nature and evolution of these sources. The high-luminosity end ($L_X >$ several 10^{37} ergs s^{-1}) of the XLF is now well constrained from the study of many E and S0 galaxies observed with *Chandra* (e.g., Kim & Fabbiano 2004; Gilfanov 2004). The normalization (i.e., the total number of LMXBs in a given galaxy) is strongly related to the stellar mass of the galaxy (Gilfanov 2004; see also Kim & Fabbiano 2004), as would be expected in the case of slowly evolving LMXBs, although a link to the specific frequency of GCs has also been reported (Kundu et al. 2002; Kim & Fabbiano 2004; Kim et al. 2006a). As first suggested by Sarazin et al. (2001), the XLF may be broken, possibly reflecting the presence of both neutron star and black hole LMXBs in the X-ray source populations (Ivanova & Kalogera 2006). However, Kim & Fabbiano (2004) found that the break occurs at a higher luminosity, $L_X = (5 \pm 1.6) \times 10^{38}$ ergs s^{-1} (with an error at 90%; see also Gilfanov 2004). Although the break luminosity is still consistent (within a 3 σ error) with the Eddington luminosity (2×10^{38} ergs s^{-1}) of a 1.4 $M_\odot$ neutron star, the best-fit value is close to the Eddington luminosity of either He-enriched accretion or a massive neutron star ($\sim 3\,M_\odot$). This break is also predicted in the model of short-lived, high-birth-rate, ultracompact binary evolution in GCs by Bildsten & Deloye (2004).

What has been less well constrained so far is the behavior of the XLF at lower luminosities, which are more typical of the majority of LMXBs in the bulge of the Milky Way and M31. With the exception of NGC 5128 (the radio galaxy Centaurus A), for which the XLF has been measured down to $\sim 2 \times 10^{36}$ ergs s^{-1} (Kraft et al. 2001; Voss & Gilfanov 2006), the available *Chandra* data so far have not allowed the detection of LMXBs in E and S0 galaxies at luminosities below the mid 10^{37} ergs s^{-1} range. By including Cen A and the LMXB (bulge) population of nearby spirals in a co-added XLF, Gilfanov (2004) suggested a significant flattening of the XLF at $L_X < 5 \times 10^{37}$ ergs s^{-1} (see also Voss & Gilfanov 2006). This flattening, first reported in the LMXB XLF of the Milky Way (Grimm et al. 2002), is suggested in a number of models, albeit because of different mechanisms

[1] Harvard-Smithsonian Center for Astrophysics, 60 Garden Street, Cambridge, MA 02138; kim@cfa.harvard.edu, gfabbiano@cfa.harvard.edu, azezas@cfa.harvard.edu.
[2] Northwestern University, Department of Physics and Astronomy, 2145 Sheridan Road, Evanston, IL 60208; vicky@northwestern.edu.
[3] University of Leicester, Leicester LE1 7RH, UK; ark@star.le.ac.uk.
[4] Dipartimento di Astronomia, Università di Bologna, Via Ranzani 1, 40127 Bologna, Italy; silvia.pellegrini@unibo.it.
[5] INAF–Osservatorio Astronomico di Brera, Via Brera 28, 20121 Milan, Italy; ginevra.trinchieri@brera.inaf.it.
[6] Department of Physics and Astronomy, Michigan State University, East Lansing, MI 48824-2320; zepf@pa.msu.edu.
[7] Laboratory for High Energy Astrophysics, NASA Goddard Space Flight Center, Code 660, Greenbelt, MD 20771; angelini@davide.gsfc.nasa.gov.
[8] Denys Wilkinson Building, University of Oxford, Keble Road, Oxford OX1 3RH, UK; rld@astro.ox.ac.uk.
[9] Astronomy Department, University of Wisconsin, 475 North Charter Street, Madison, WI 53706; jsg@astro.wisc.edu.

TABLE 1
BASIC INFORMATION ON THE TWO GALAXIES

Name (1)	D (Mpc) (2)	R_{25} (arcmin) (3)	PA (deg) (4)	B_{T_0} (mag) (5)	M_B (mag) (6)	L_B ($L_{B,\odot}$) (7)	S_ν (8)	N(H) (10^{20} cm^{-2}) (9)
NGC 3379.....	10.57	2.69 × 2.39	67.5	10.18	19.94	1.35E10	1.2	2.78
NGC 4278.....	16.07	2.04 × 1.90	27.5	10.97	20.06	1.63E10	6.9	1.76

NOTES.—Col. (1): Galaxy name. Col. (2): Distance, from Tonry et al. (2001). Col. (3): Optical size (diameter) of galaxy determined at 25th magnitude from RC3 (de Vaucouleurs et al. 1991). Col. (4): Position angle of the major axis from NED. Col. (5): B_{T_0} from RC3. Col. (6): Absolute blue magnitude. Col. (7): Blue luminosity calculated by adopting absolute solar blue magnitude of 5.47 mag. Col. (8): Globular cluster specific frequency from Ashman & Zepf (1998). Col. (9): H column density along the Galactic line of sight, from Dickey & Lockman (1990).

(e.g., Bildsten & Deloye 2004; Pfahl et al. 2003; Postnov & Kunanov 2005). The "outburst peak luminosity–orbital period" correlation (e.g., Fig. A1 of Portegies Zwart et al. 2004; see also Chen et al. 1997) established for black hole transients suggests that there may be a low-luminosity break due to the instability of accretion disks to transient outbursts for very short period (∼1 hr) binaries. Binaries with such tight orbits are expected to have low-mass, hydrogen-poor companions with mass transfer being driven by gravitational radiation. Such tight binaries with black hole accretors are expected to be transient (King et al. 1996), as also confirmed by observed systems (Portegies Zwart et al. 2004). Similarly, as discussed by Bildsten & Deloye (2004) ultracompact LMXBs with neutron star accretors predominantly form in GCs and would show a break at $\sim 10^{37}$ ergs s^{-1} in the absence of X-ray heating, while with X-ray heating the disk can remain stable to lower luminosities, so no XLF break would occur. It is therefore important to study the low-luminosity XLF of normal elliptical LMXB populations to confirm the presence and ubiquity of this break. Moreover, detailed studies of the globular cluster LMXB population of M31 have reported a distinctive break at $\sim 2 \times 10^{37}$ ergs s^{-1} (Kong et al. 2003; Trudolyubov & Priedhorsky 2004). The discovery of a similar break in the E and S0 XLFs may argue for a GC-LMXB connection in these galaxies.

In this paper we report the first direct measurement of the low-luminosity XLF in normal nearby elliptical galaxies. The two galaxies NGC 3379 and NGC 4278 (Table 1) are being observed as part of a *Chandra* very large program (for 340 and 500 ks, respectively) to study in depth the LMXB population. Because both elliptical galaxies are old (e.g., Trager et al. 2000; Terlevich & Forbes 2002), they provide a clean sample of LMXBs with no contamination by HMXBs, which are likely to contribute to the X-ray source populations of spiral galaxies (the Milky Way and M31) and young or rejuvenated E and S0 galaxies resulting from recent mergers (e.g., NGC 5128). While we expect to reach a limiting luminosity of a few $\times 10^{36}$ ergs s^{-1} at the end of this observing campaign, our first observations, in conjunction with the data in the *Chandra* archive, result in total exposures of 110 and 140 ks, respectively. The corresponding limiting luminosities, restricting ourselves to data not affected by incompleteness, are 1 and 3×10^{37} ergs s^{-1} (for NGC 3379 and NGC 4278, respectively); applying incompleteness corrections to the data, the resulting XLFs reach down to $\sim 5 \times 10^{36}$ and $\sim 1 \times 10^{37}$ ergs s^{-1}, respectively. As discussed in this paper, we find that the conclusion of a ubiquitous flattening of the XLF is not supported by our results.

We adopt distances of 10.6 Mpc (NGC 3379) and 16.1 Mpc (NGC 4278) throughout this paper, based on the surface brightness fluctuation analysis by Tonry et al. (2001). At these distances, $1'$ corresponds to 3.1 and 4.7 kpc, respectively.

2. *CHANDRA* X-RAY OBSERVATIONS

NGC 3379 was observed for 85 ks on 2006 January 23 with the S3 (back-illuminated) chip of *Chandra* Advanced CCD Imaging Spectrometer (ACIS) (ObsID 7073). The ACIS data were reduced in a manner similar to that described in Kim & Fabbiano (2003) with a custom-made pipeline (XPIPE), specifically developed for the *Chandra* Multiwavelength Project (ChaMP; Kim et al. 2004a). Removal of background flares reduced the effective exposure time of CCD S3 to 80 ks. NGC 3379 had been previously observed with *Chandra* ACIS (ObsID 1587) for 29 ks on 2001 February 13 (David et al. 2005). We have retrieved these data from the *Chandra* archive[10] and reduced them with the same method after correcting instrumental effects (e.g., time-dependent QE variation) with up-to-date calibration data.[11] Combining the two observations by reprojecting to a common tangent point,[12] we reach an effective exposure on CCD S3 of 110 ks. We show the merged image in Figure 1 (*left*), where the X-ray point sources and the optical size (D_{25}) are marked.

NGC 4278 was observed for 110 ks on 2006 March 16 with the S3 chip of ACIS (ObsID 7077). Removal of background flares reduced the effective exposure time to 108 ks. NGC 4278 had been previously observed with ACIS (ObsID 4741) for 37 ks on 2005 February 3 (PI: J. Irwin). We have also combined the two observations, and the merged data correspond to an effective exposure on CCD S3 of 145 ks. The merged image is shown in Figure 1 (*right*).

3. X-RAY LUMINOSITY FUNCTIONS

From the merged images of the NGC 3379 and NGC 4278 observations, we detect 109 and 197 point sources in CCD S3 only (Table 2, col. [5]). A number of these sources vary, and some are detected only in one observation. Source variability and spectral parameters will be presented in a future paper. In this paper, we only consider the effect of source variability on the observed XLF. To measure the X-ray luminosity (in 0.3–8 keV) from the merged data, we take into account the temporal QE variation[13] by calculating the energy conversion factor (ECF) in each observation and then taking an exposure-weighted mean ECF. The ECF (0.3–8 keV) varies by ∼12% between the two observations of NGC 3379 and by 0.1% between the two observations of NGC 4278. We assume a power-law spectral model with a photon index of 1.7 and the Galactic absorption (see Table 1).

To construct the XLF, we use point sources detected within the D_{25} ellipse (the size and position angle are given in Table 1).

[10] See http://asc.harvard.edu/cda.
[11] See http://asc.harvard.edu/caldb.
[12] Using `merge_all`, which is available in the CIAO contributed package; see http://cxc.harvard.edu/ciao/threads/combine.
[13] See http://cxc.harvard.edu/cal/Acis/Cal_prods/qeDeg.

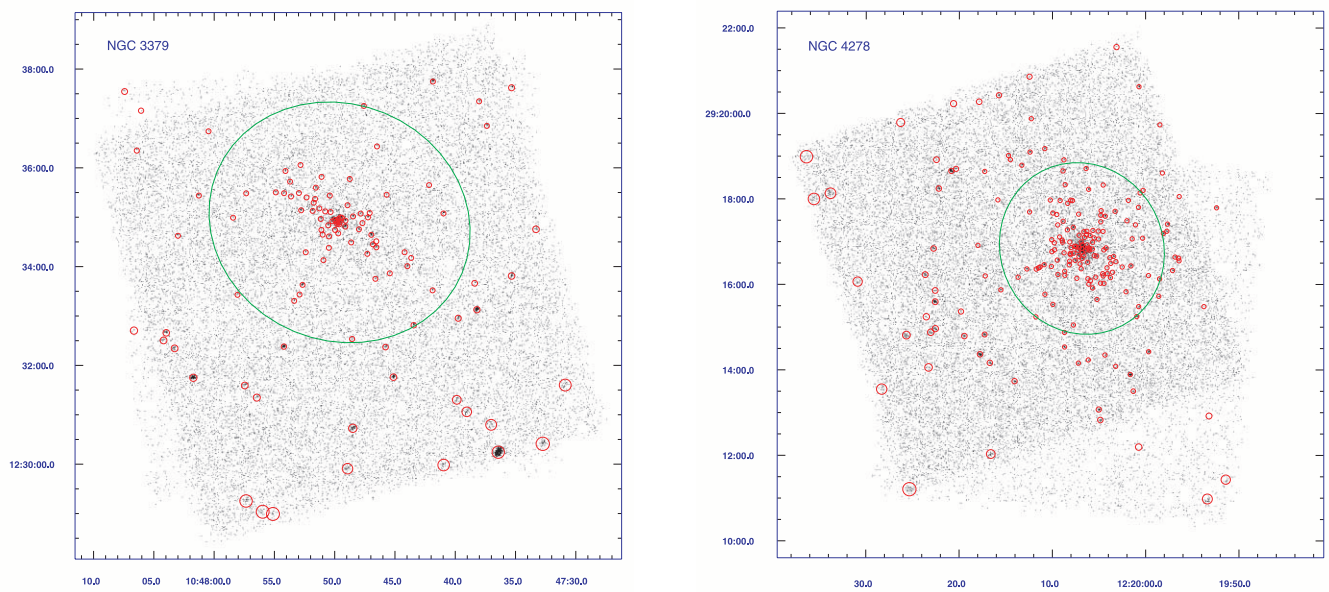

FIG. 1.—Merged *Chandra* images of NGC 3379 (*left*) and NGC 4278 (*right*). The large green ellipse indicates the optical galaxy size at the 25th magnitude, and the small circles indicate detected point sources.

Although some X-ray sources outside the D_{25} ellipse may be associated with the galaxy, we exclude them to reduce the contamination by foreground or background X-ray sources. Based on the ChaMP+CDF $\log N - \log S$ relation (Kim et al. 2006b), we estimate the cosmic background sources (mostly AGNs) to be 4–13 (Table 2, col. [10]) within the D_{25} ellipse at the flux limit of 90% completeness (Table 2, col. [8]; see below for details). This results in a source contamination of 20% in NGC 3379 and 7% in NGC 4278 (see also Fig. 2); these fractions would be considerably higher if we included the sources detected outside the D_{25} ellipse, since they scale with the search area. We also exclude sources located near the galactic centers ($R < 10''$), because of the large photometric error caused by confusion with other overlapping sources and by the presence of diffuse emission; these conditions make the incompleteness corrections uncertain. In a previous work with 14 elliptical galaxies, Kim & Fabbiano (2004) excluded sources within $R < 20''$ from the XLF; the smaller amount of hot ISM present in both NGC 3379 and NGC 4278 allows us to use sources nearer to the galaxy centers in this case. With these selection criteria, we obtain 59 and 112 sources in NGC 3379 and NGC 4278, respectively, to build the XLFs.

To determine the XLFs accurately, it is most critical to correct for incompleteness (see Kim & Fabbiano 2003, 2004). Without such correction, the XLF would look flattened at the lower luminosities where the detection is not complete, causing an artificial break. Following Kim & Fabbiano (2004), we performed extensive simulations to generate incompleteness corrections: we simulated 20,000 point sources using MARX,[14] added them one by one to the observed image, and then determined whether the added source is detected. Since we used the real observed data as the baseline, we could correct simultaneously three biases: detection limit, Eddington bias (Eddington 1913), and source confusion (Kim & Fabbiano 2003). In the simulations, we assumed a typical LMXB XLF differential slope of $\beta = 2$ (Kim & Fabbiano 2004),

$$\frac{dN}{dL_X} = kL_X^{-\beta}.$$

[14] See http://space.mit.edu/ASC/MARX.

TABLE 2

Chandra OBSERVATIONS OF THE TWO GALAXIES

NAME	OBSID	OBS. DATE	NET EXPOSURE	NUMBER OF SOURCES			90% COMPLETENESS LIMIT		NUMBER OF BACKGROUND SOURCES	SLOPE	AMPLITUDE
			(ks)	S3	D_{25}	$R > 10''$	F_X	L_X			
(1)	(2)	(3)	(4)	(5)	(6)	(7)	(8)	(9)	(10)	(11)	(12)
NGC 3379.....	01587	2001 Feb 13	28.8	72	44	34	1.5E−15	2.1E37	8	1.8 ± 0.3	7.5 ± 2.6
	07073	2006 Jan 23	80.3	86	57	45	0.9E−15	1.3E37	12	1.8 ± 0.2	6.2 ± 2.2
	Merge	...	109.9	109	70	59	0.8E−15	1.0E37	13	1.9 ± 0.2	5.6 ± 1.8
NGC 4278.....	04741	2005 Feb 3	36.6	92	58	54	2.2E−15	6.5E37	4	1.9 ± 0.2	22.9 ± 4.1
	07077	2006 Mar 16	107.6	175	116	108	1.1E−15	3.3E37	7	2.0 ± 0.1	23.2 ± 4.6
	Merge	...	144.6	197	122	112	0.9E−15	2.8E37	8	1.9 ± 0.1	23.1 ± 4.4

NOTES.—Col. (1): Galaxy name. Col. (2): *Chandra* observation ID. Col. (3): *Chandra* observation date. Col. (4): Net exposure after removing the background. Col. (5): Number of point sources detected in CCD S3. Col. (6): Number of point sources detected within the D_{25} ellipse. Col. (7): Same as col. (6), but excluding sources at $R < 10''$. These sources are actually used in building the XLF. Col. (8): The 90% completeness limit in the source flux (0.3–8 keV); i.e., 10% of sources with this flux would not be detected inside the D_{25} ellipse, but excluding the central $10''$. Col. (9): Same as col. (8), but in the source luminosity (0.3–8 keV). Col. (10): Number of cosmic background sources within the D_{25} ellipse at the flux limit given in col. (8). Col. (11): Best-fit XLF slope (in a differential form) and error (90% confidence). Col. (12): Best-fit XLF amplitude and error (90% confidence).

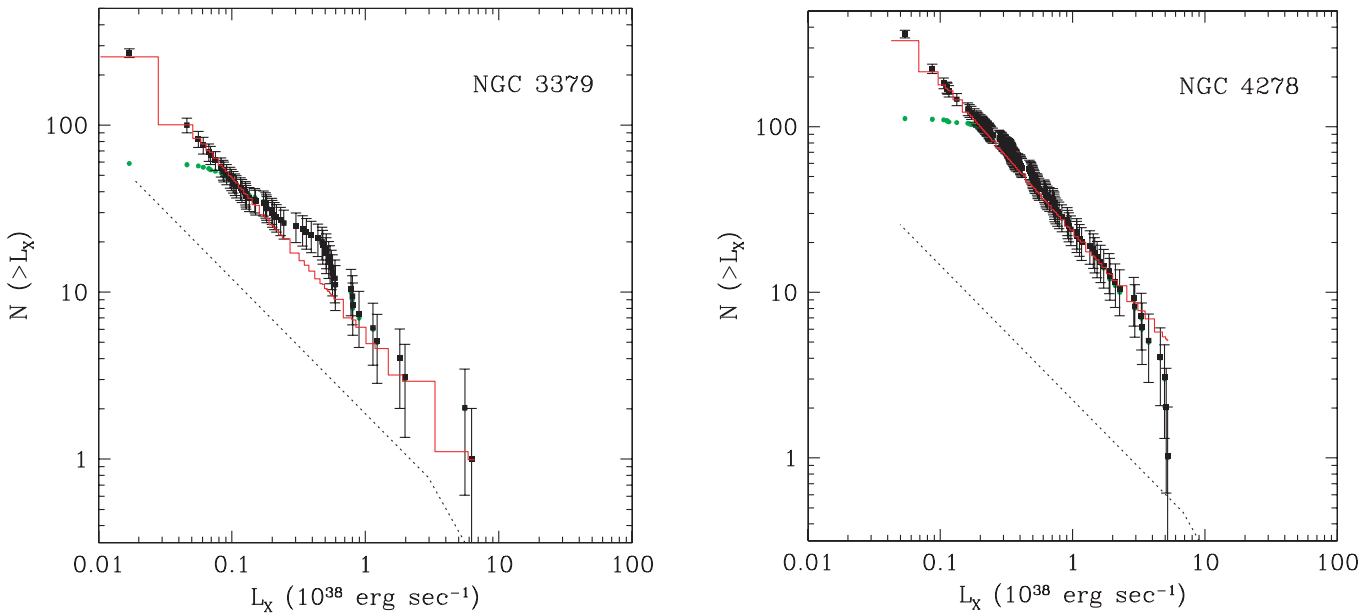

FIG. 2.—X-ray luminosity function of LMXBs determined with the merged observations of NGC 3379 (*left*) and NGC 4278 (*right*). Filled squares with error bars indicate the bias-corrected XLF, and green circles indicate the raw data. The best-fit single-power-law model is plotted by the histogram. The dotted line indicates the expected number of cosmic X-ray background sources determined with the ChaMP+CDF data (Kim et al. 2006a).

We note that the adopted XLF slope does not significantly affect the results, because the correction is determined by the ratio of the number of input sources to that of detected sources (see also Kim & Fabbiano 2003). As shown in Kim et al. (2006a), the radial distribution of LMXBs closely follows that of the optical halo light, regardless of their association with globular clusters. Therefore, we adopted an $r^{-1/4}$ law for the radial distribution of the LMXBs. Also, we did not use LMXBs in the central regions, where the radial profile dependency is most significant.

We find that the 90% completeness limit (i.e., where 10% of sources with this luminosity would not be detected inside the D_{25} ellipse, but excluding the central 10″) is $L_X = 1 \times 10^{37}$ ergs s^{-1} for NGC 3379 and $L_X = 3 \times 10^{37}$ ergs s^{-1} for NGC 4278 (Table 2, col. [9]); we can reliably correct the XLFs to X-ray luminosities at least a factor of 2–3 lower than the 90% limit (roughly corresponding to a 50% limit).

We show the bias-corrected cumulative XLFs in Figure 2, where the corrected data are identified by squares with error bars and the uncorrected raw data by smaller circles. It is clear that the apparent XLF flattenings at low luminosities disappear in both cases. Using Sherpa,[15] we fit the bias-corrected XLFs (in a differential form) with single power laws using Cash statistics (for an unbinned distribution, but read in Sherpa as a histogram mode) and χ^2 statistics (for a binned distribution). The Cash statistic utilizes a maximum likelihood function and can be applied regardless of the number in each bin. For the χ^2 statistics, we select the minimum to be 10 sources in each bin and apply the Gehrels variance function for the error calculation (Gehrels 1986). Both statistics result in consistent parameters within the errors. The solid lines in Figure 2 indicate the best-fit single-power-law models determined with the Cash statistics. We list the best-fit parameters and the corresponding errors (90% confidence level) in Table 2. As indicated in Figure 2, the quality of fitting with a single power law is good. The χ^2 method results in $\chi^2_{\rm red} = 1.19$ with 4 degrees of freedom (dof) and $\chi^2_{\rm red} = 0.70$ with 10 dof for NGC 3379 and NGC 4278, respectively. To check the possible XLF flattening at low luminosities, we applied a broken power law with the break luminosity varying freely. In both galaxies, a slightly improved total χ^2 accompanied by a lower dof value resulted in a worse $\chi^2_{\rm red}$. Based on the F-test, the corresponding null hypothesis probability is 0.3 (0.5) for NGC 3379 (NGC 4278), indicating that the broken power law is not statistically required with the given luminosity range. We also fitted the data excluding the faint sources below the 50% completeness limit, reaching consistent results within the statistical errors. In NGC 3379, there is an excess over the best-fit power law at $L_X = (3\text{–}6) \times 10^{37}$ ergs s^{-1}, but its significance is only marginal ($\sim$1.6 σ).

Also plotted in Figure 2 is the expected number (*dotted line*) of cosmic X-ray background sources (Kim et al. 2006b). Because background sources are not fully detected at low fluxes (the same detection incompleteness as for the sources in the galaxies would apply), the dotted line would be as flattened as the observed XLF; therefore the dotted line should be compared with the corrected XLF. It is then clear that the contamination is only a small fraction (20% in NGC 3379 and 7% in NGC 4278) and that the steepening at low L_X is not due to background source contamination. We repeated the XLF fit with an additional power-law component for the expected background sources and obtained best-fit parameters consistent with those listed in Table 2.

We further check whether our results (particularly for NGC 3379) might be affected by the field-to-field variation of cosmic X-ray background sources, as expected from the large-scale structure of the universe, although the observational evidence is still controversial (e.g., see a review by Brandt & Hasinger 2005). Kim et al. (2004b) extensively compared field-to-field number counts with the ChaMP data and found no statistically significant evidence for cosmic variance at $F_X > 10^{-15}$ ergs s^{-1} cm^{-2} with a possible 10%–20% chip-to-chip variation among those observations with an exposure (60–130 ks). Even if a smaller region corresponding to the D_{25} ellipse of NGC 3379 ($\sim\frac{1}{3}$ of a single chip area) is considered, the variation is still less than 30%. Simultaneously analyzing CDF-N and S data, Bauer et al. (2004) concluded, in contrast to earlier reports (e.g., Rosati et al. 2002), that the number counts of the two CDFs are consistent with each

[15] See http://cxc.harvard.edu/sherpa.

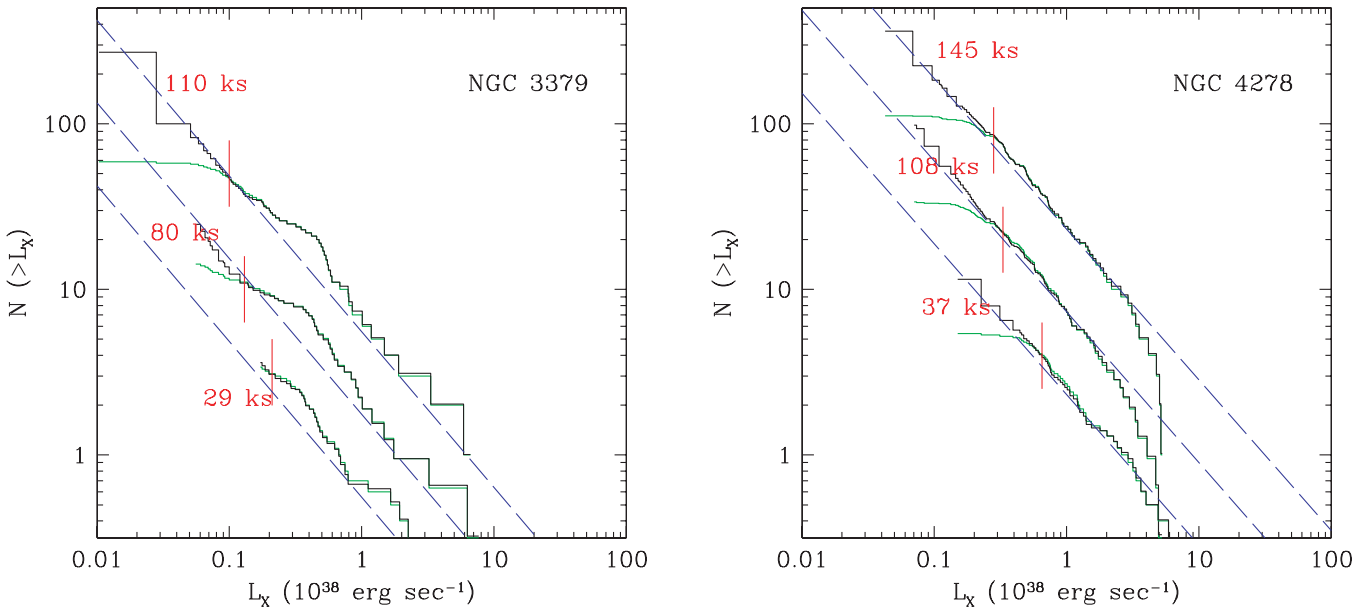

FIG. 3.—XLFs determined with two individual observations are compared with that of the merged observation. The black and green histograms indicate the corrected and uncorrected XLFs. The vertical bar indicates a 90% completeness limit (Table 2, col. [9]). The XLFs determined in two individual observations are shifted down vertically by $\Delta \log N = -1.0$ (the shallower one) and -0.5 (the deeper one). The best-fit single-power-law model (*dashed blue diagonal lines*) determined with the merged observations is plotted with observed XLFs (for both individual and merged observations).

other down to the detection limit (a few $\times 10^{-17}$ ergs s^{-1} cm^{-2}) in the soft band (0.5–2.0 keV) and to $F_X = 10^{-15}$ ergs s^{-1} cm^{-2} in the hard band (2–8 keV). The statistically significant variance is only seen for faint sources ($F_X > 10^{-15}$ ergs s^{-1} cm^{-2}) in the hard band, likely due to heavily obscured sources (see also Yang et al. 2003). We note that $F_X = 10^{-15}$ ergs s^{-1} cm^{-2} is close to the 90% detection limit for NGC 3379 and corresponds to $L_X = 1.4 \times 10^{37}$ ergs s^{-1}, well below the reported XLF break. To estimate quantitatively the variance on a galactic scale, we repeatedly count the number of sources with $F_X > 10^{-15}$ ergs s^{-1} cm^{-2} within the area of the D_{25} ellipse of NGC 3379 by randomly selecting the location within the CDF field of view. The 1 σ rms deviation from the mean is ~30% of the mean, similar to the ChaMP result. Unless the cosmic variance is accompanied by a considerably steeper $\log N - \log S$ slope (this is opposite to the flatter slope for the more obscured hard-band sources found by Bauer et al. [2004]), the 30% cosmic variation from the ~20% background sources would not change our result (see Fig. 2). The spatial concentration of point sources toward the galactic center and their mostly unabsorbed spectral properties (e.g., G. Fabbiano et al. 2006, in preparation) also confirms that the background sources cannot dominate. Furthermore, the number of point sources in NGC 3379 is already low for its total optical luminosity (see § 4); hence this galaxy would be rather unusual if a significant fraction of point sources were background sources.

To investigate the effect of source variability on the XLFs, we compare XLFs built from the individual observations (as well as the merged observations) in Figure 3. The black and green histograms indicate the corrected and uncorrected XLFs, respectively. The vertical bars mark the 90% completeness limits (Table 2, col. [9]). The XLFs from the two individual observations are shifted downward vertically by $\Delta \log N = -1.0$ (the shallower one) and -0.5 (the deeper one) for visibility. Error bars are not plotted here to avoid overcrowding, but can be seen in Figure 2 for the merged XLFs. The best-fit single-power-law models (*dashed blue diagonal lines*) determined from the merged observations are plotted with the XLFs (both individual and merged). In general, the XLFs (both in slope and amplitude) are consistent with each other, within the statistical error, even though there are a number of variable X-ray sources. A similarly robust XLF in multiple observations of the Antennae was previously reported (Zezas 2006). However, we caution that using merged observations spanning a few years, we are not directly measuring the peak luminosity or the luminosity averaged over an outburst cycle, which is more useful for constraining the binary evolution model.

The validity of our low-luminosity bias correction is also verified by comparing the XLFs made from observations of different depths. The corrected XLFs from the shallower observations closely follow the XLFs from the deeper observations at low luminosities. This is most clearly seen in NGC 4278, which hosts a larger number of LMXBs and hence has a higher statistical significance (Fig. 3, *right*). The predicted (corrected) XLF below $L_X < 6.5 \times 10^{37}$ ergs s^{-1} (the 90% confidence limit) of the 37 ks observation (ObsID 04741) is well reproduced in the observed (uncorrected) XLF of 108 ks observation (ObsID 07077) down to $L_X < 3 \times 10^{37}$ ergs s^{-1}.

The high-luminosity shape of the XLF of the LMXB populations of elliptical galaxies is well established with a large sample of elliptical galaxies and can be fitted with a broken-power-law model, with a break (at 5×10^{38} ergs s^{-1}; Kim & Fabbiano 2004; Gilfanov 2004) that may stem from the presence of neutron star and black hole binary populations. In the current sample, we cannot constrain the high-luminosity break because of a small number of luminous sources (only two sources in each galaxy with $L_X > 5 \times 10^{38}$ ergs s^{-1}). We also note that in NGC 4278 (Fig. 3, *right*), the XLF of the longer observation (ObsID 7077) looks steeper in the high L_X range than that of the shorter observation (ObsID 4741), but this is simply because the most luminous source ($L_X = 2 \times 10^{39}$ ergs s^{-1}), seen in the shorter (earlier) observation, disappears in the longer observation taken a year later.

4. DISCUSSION

In this paper, for the first time we explore the low-luminosity XLFs of normal elliptical galaxies. This low-luminosity XLF has

been studied in the Galaxy, where a flattening at low luminosities has been reported (Grimm et al. 2002), and in M31, where diverse and complex behavior can be seen looking at different stellar fields (e.g., Kong et al. 2002, 2003; Trudolyubov & Priedhorsky 2004; see review in Fabbiano & White 2006). Gilfanov (2004) suggested that a low-luminosity flattening of the LMXB XLF is a general feature of LMXB populations. This flattening is also observed in the X-ray source population of NGC 5128 (Cen A), below $L_X = 5 \times 10^{37}$ ergs s^{-1} (Voss & Gilfanov 2006).

Our results suggest that the conclusion of a ubiquitous flattening of the low-luminosity shape of the LMXB XLF may be premature. In two normal elliptical galaxies, NGC 3379 and NGC 4278, we found that the XLFs can be fitted with a single-power-law differential slope $\beta = 1.9 \pm 0.1$, comparable with the average XLF of other elliptical galaxies (Kim & Fabbiano 2004). In NGC 4278 we find that the XLF follows this single power law down to the 90% completeness limit of 3×10^{37} ergs s^{-1}, and that this trend extends down to 10^{37} ergs s^{-1} in the bias-corrected XLF. In NGC 3379, there could be a break at $\sim 4 \times 10^{37}$ ergs s^{-1} (although the discrepancy from a single-power-law fit is only a 1.6 σ effect), but the XLF becomes steep again below 2×10^{37} ergs s^{-1} and follows this shape at least down to $\sim 5 \times 10^{36}$ ergs s^{-1}. We can exclude this steep power law at low luminosities being the result of some problem with our bias correction, because it is directly observed in the complete portion of the merged XLF (see Fig. 3). In summary, our results show that there is no universal flattening of the XLF at low luminosities.

We note that although a flattening was reported in the XLF of NGC 5128, there are several concerns that may affect these results, although the authors (Voss & Gilfanov 2006) tried to take them into account. NGC 5128 is far from being a normal elliptical, since its X-ray source population may have been rejuvenated by a merger event, and mixing with a population of HMXBs (which is known to have a shallower XLF; e.g., Grimm et al. 2002) is possible; HMXB contamination may also affect the XLFs of the Milky Way and M31. Also, the X-ray emission of NGC 5128 is complex, with various substructures in the hot ISM as well as strong dust lanes, optical filaments, radio/X-ray jets, etc. (e.g., Karovska et al. 2002), potentially increasing the difficulty of obtaining a bias-free low-luminosity XLF. Moreover, the large angular size ($D_{25} = 26'$) of NGC 5128 makes it hard to effectively remove contamination by foreground and background X-ray sources, which, given the depth of the exposure, account for about half of the detected sources (Voss & Gilfanov 2006). We note that at the distance of NGC 5128 (3.5 Mpc), the break in the cosmic X-ray background $\log N - \log S$ relation at $F_X \sim 2.5 \times 10^{-14}$ ergs s^{-1} cm^{-2} (Kim et al. 2006b) happens to correspond to $L_X \sim 4 \times 10^{37}$ ergs s^{-1}, close to the reported break.

Many models predict that the LMXB XLF should flatten at low luminosities, although the exact break luminosity is not well determined (see review by Fabbiano 2006). Flattening of the XLF is found in the population synthesis of field LMXBs of Pfahl et al. (2003, their Fig. 3), if irradiation of the donor star from the X-ray emission of the compact companion is considered in the model. The model of Bildsten & Deloye (2004) of formation of ultracompact LMXBs in GCs also predicts a flattening at lower luminosities ($L_X \sim 10^{37}$ ergs s^{-1}), where these sources would become transient and therefore disappear from the XLF, but this break may also occur at much lower luminosities if X-ray heating stabilizes the accretion disk (see also Deloye & Bildsten 2003). In this light, we note that if the possible XLF bump, or break, at $L_X \sim 4 \times 10^{37}$ ergs s^{-1} in NGC 3379 is real, this (and the absence of the XLF break in NGC 4278) could suggest a higher fraction

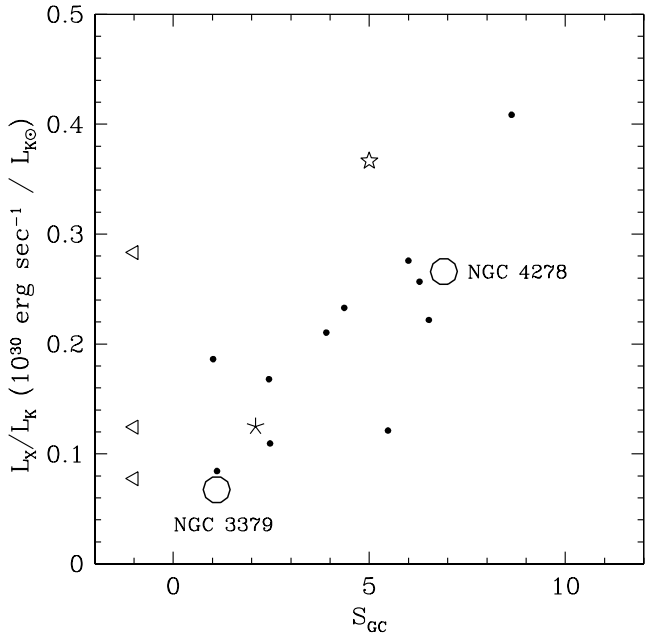

FIG. 4.—L_X(LMXB)/L_K plotted against the GC specific frequency, S_ν. Our two galaxies, NGC 3379 and NGC 4278, are overplotted on the scatter plot taken from Kim & Fabbiano (2004) to indicate that the large difference in L_X(LMXB) is consistent with the general trend between L_X(LMXB)/L_K and S_ν. Three galaxies with no S_ν are marked with triangles on the left side of the figure. Also plotted are the bulges of the Milky Way (*star*) and M31 (*asterisk*).

of ultracompact, X-ray-heating-stabilized, low-luminosity sources in NGC 4278, consistent with the higher GC specific frequency (S_ν) of this galaxy (see Table 2). More recently, Postnov & Kuranov (2005) argue that a low-luminosity break would be related to different accretion driving mechanisms in LMXBs: in the lower luminosity sources ($L_X <$ a few $\times 10^{37}$ ergs s^{-1}) accretion may be driven by angular momentum removal by gravitational waves, while at higher luminosities (a few $\times 10^{37}$ ergs s$^{-1} < L_X < 5 \times 10^{38}$ ergs s^{-1}) magnetic stellar winds may be responsible. Optical identification of X-ray sources with GCs and an estimate of the transient fraction at different luminosities (which we will attempt once the full body of observations of NGC 3379 and NGC 4278 are completed) may help discriminate among possible scenarios.

It cannot be excluded that there are differences in the XLFs of different LMXB populations, possibly reflecting different origins of these LMXBs. Even ignoring the possible bump in NGC 3379, while the XLF slopes of our two galaxies are similar, their amplitudes (i.e., total LMXB X-ray luminosity or total number of LMXBs) differ by a factor of 4 (Table 2). This in turn results in a factor of 4 difference in L_X(LMXB)/L_K. Because their optical luminosities are similar (Table 1), this discrepancy is not related to the total stellar mass, which has been suggested as the main driver of the normalization of the LMXB XLF (Gilfanov 2004). This discrepancy is of the order of the maximum amount of the scatter observed in the relation between the X-ray luminosity of LMXBs and the optical luminosity in 14 early-type galaxies by Kim & Fabbiano (2004). In our two galaxies, the GC specific frequency (S_ν) is different, NGC 4278 having a considerably higher S_ν than NGC 3379 (Fig. 4; Table 1, col. [8]). This is then in a good agreement with the general trend of a positive correlation between L_X(LMXB)/L_K and S_ν found with a larger sample in Kim & Fabbiano (2004), indicating that a significant number of LMXBs have originated predominantly in globular clusters, particularly in NGC 4278. The LMXB-GC connection and the

comparison between field and GC LMXBs will be explored in a future paper.

5. CONCLUSIONS

We have derived and analyzed the deepest XLF of LMXBs in two normal old-stellar-population elliptical galaxies: NGC 3379 and NGC 4278. The XLF of NGC 4278 reaches down to 1×10^{37} ergs s^{-1} and follows closely a straight, unbroken power law of differential slope 1.9 ± 0.1, with high statistical significance. This result shows that the "universal" break of the LMXB XLF at $\sim 5 \times 10^{37}$ ergs s^{-1}, suggested by Gilfanov (2004), is not universal. The XLF of NGC 3379 is also well fitted by a similar power law, although there is a possible ($1.6\,\sigma$) excess above this power law at $\sim 4 \times 10^{37}$ ergs s^{-1}. Even if this excess is real, it may not represent a break, because the power law resumes at lower luminosities, below $\sim 2 \times 10^{37}$ ergs s^{-1}.

Comparison of the normalizations of the XLFs (i.e., the integrated LMXB luminosities of the galaxies) shows that for the same integrated stellar luminosity, NGC 4278 is $\sim$4 times overluminous in X-rays. This results confirms the conclusion of Kim & Fabbiano (2004; see also White et al. 2002) that although stellar luminosity/mass is an important driver of XLF normalization, as suggested by Gilfanov (2004), it is not the sole driver. The specific frequency of globular clusters in a galaxy is also important: while NGC 3379 has few GCs, NGC 4278 is GC-rich.

This paper is the first report on the deep XLF study of LMXB populations that is being currently performed with a *Chandra* very large program. Future work will push these XLFs to even lower luminosities and will explore separately the contributions of field and GC LMXBs to the XLF.

This work was supported by *Chandra* GO grant G06-7079A (PI: Fabbiano) and subcontract GO6-7079B (PI: Kalogera). D.-W. Kim acknowledges support from NASA contract NAS8-39073 (CXC); A. Zezas acknowledges support from NASA LTSA grant NAG5-13056. The data analysis was supported by the CXC CIAO software and CALDB.

REFERENCES

Ashman, K. M., & Zepf, S. E. 1998, Globular Cluster Systems (Cambridge: Cambridge Univ. Press)
Bauer, F. E., et al. 2004, AJ, 128, 2048
Bildsten, L., & Deloye, C. J. 2004, ApJ, 607, L119
Brandt, W. N., & Hasinger, G. 2005, ARA&A, 43, 827
Chen, W., Shrader, C. R., & Livio, M. 1997, ApJ, 491, 312
David, L. P., Jones, C., Forman, W., & Murray, S. 2005, ApJ, 635, 1053
Deloye, C. J., & Bildsten, L. 2003, ApJ, 598, 1217
de Vaucouleurs, G., et al. 1991, Third Reference Catalogue of Bright Galaxies (New York: Springer)
Dickey, J. M., & Lockman, F. J. 1990, ARA&A, 28, 215
Eddington, A. S. 1913, MNRAS, 73, 359
Fabbiano, G. 2006, ARA&A, 44, 323
Fabbiano, G., & White, N. 2006, in Compact Stellar X-Ray Sources, ed. W. H. G. Lewin & M. van der Klis (Cambridge: Cambridge Univ. Press), 475
Gehrels, N. 1986, ApJ, 303, 336
Gilfanov, M. 2004, MNRAS, 349, 146
Grimm, H.-J., Gilfanov, M., & Sunyaev, R. 2002, A&A, 391, 923
Grindlay, J. E. 1984, Adv. Space Res., 3, 19
Irwin, J. 2005, ApJ, 631, 511
Ivanova, N., & Kalogera, V. 2006, ApJ, 636, 985
Karovska, M., et al. 2002, ApJ, 577, 114
Kim, D.-W., & Fabbiano, G. 2003, ApJ, 586, 826
———. 2004, ApJ, 611, 846
Kim, D.-W., et al. 2004a, ApJS, 150, 19
———. 2004b, ApJ, 600, 59
Kim, E., et al. 2006a, ApJ, 647, 276
Kim, M., et al. 2006b, ApJ, submitted
King, A. R., Kolb, U., & Burderi, L. 1996, ApJ, 464, L127
Kong, A., et al. 2002, ApJ, 577, 738
———. 2003, ApJ, 585, 298
Kraft, R. P., et al. 2001, ApJ, 560, 675
Kundu, A., Maccarone, T. J., & Zepf, S. E. 2002, ApJ, 574, L5
Maccarone, T. J., Kundu, A., & Zepf, S. E. 2003, ApJ, 586, 814
Pfahl, E., Rappaport, S., & Podsiadlowski, Ph. 2003, ApJ, 597, 1036
Portegies Zwart, S. F., Dewi, J., & Maccarone, T. 2004, MNRAS, 355, 413
Postnov, K. A., & Kuranov, A. G. 2005, Astron. Lett., 31, 7
Rosati, P., et al. 2002, ApJ, 566, 667
Sarazin, C. L., Irwin, J. A., & Bregman, J. N. 2001, ApJ, 556, 533
Terlevich, A. I., & Forbes, D. A. 2002, MNRAS, 330, 547
Tonry, J. L., et al. 2001, ApJ, 546, 681
Trager, S. C., et al. 2000, AJ, 119, 1645
Trudolyubov, S., & Priedhorsky, W. 2004, ApJ, 616, 821
Verbunt, F., & Lewin, W. H. G. 2006, in Compact Stellar X-Ray Sources, ed. W. H. G. Lewin & M. van der Klis (Cambridge: Cambridge Univ. Press), 341
Voss, R., & Gilfanov, M. 2006, A&A, 447, 71
White, R. E., III, Sarazin, C. L., & Kulkarni, S. R. 2002, ApJ, 571, L23
Yang, Y., et al. 2003, ApJ, 585, L85
Zezas, A. 2006, in IAU Symp. 230, Populations of High Energy Sources in Galaxies, ed. E. J. A. Meurs & G. Fabbiano (Cambridge: Cambridge Univ. Press), 369